

# Grid Connected PV Systems for Highly Efficient Performance of Constant Power Generation

Heenali Korgaonkar<sup>1</sup>, Janki Pawaskar<sup>2</sup>, Pratik Rane<sup>3</sup>, Cajetan Gonsalvis<sup>4</sup>

<sup>1,2,3,4</sup> Assistant Professor, Electronics and Telecommunication, Metropolitan Institute of Technology and Management, Sindhudurg, Maharashtra, India

DOI: 10.5281/zenodo.20610116

## ABSTRACT

*A fast and smooth transition between Maximum Power Point Tracking (MPPT) and Constant Power Generation (CPG) is ensured using an advanced power control strategy that limits the maximum feed-in power of PV systems. High-performance and stable operation are achieved regardless of the solar irradiance levels. The PV output power is regulated to any desired set-point and operates on the left side of the maximum power point without causing stability problems. The operational principle of the P&O-CPG algorithm applied to a two-stage single-phase grid-connected PV system is described to achieve stable CPG operation. The effectiveness of the proposed CPG control strategy is verified in terms of high accuracy, fast dynamic response, and stable transitions.*

**Keywords:** PV systems, power converters, constant power control, maximum power point tracking.

## 1. INTRODUCTION

To maximize energy yield in PV systems, **Maximum Power Point Tracking (MPPT)** is essential. However, advanced control strategies are needed to prevent issues like grid overloading due to high PV penetration. According to the Renewable Energy Sources Act, PV systems below 30 kWp must limit feed-in power unless controlled by utilities. This is achieved through **Constant Power Generation (CPG)** control. CPG is implemented by modifying the MPPT algorithm at the inverter level. When PV power ( $P_{pv}$ ) is below the set limit ( $P_{limit}$ ), the system operates in normal MPPT mode. However, when the output power reaches  $P_{limit}$ , the output power of the PV system is constant, i.e.,  $P_{pv} = P_{limit}$ , and leading to a constant active power injection as shown in (1) and illustrated in Fig. 1.

$$P_{PV} = P_{MPPT}, \text{ when } P_{PV} \leq P_{LIMIT} \text{ ---- } \dots \dots (1) \quad P_{PV} = P_{LIMIT}, \text{ when } P_{PV} > P_{LIMIT}$$

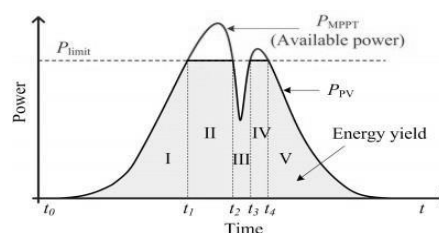


**Fig. 1.** Constant Power Generation (CPG) concept:

1) MPPT mode during I, III, V, and 2) CPG mode during II, IV

## 2. METHODOLOGY

In single stage grid connected PV systems [7], the CPG based on a Perturb and Observe (P&O-CPG) algorithm was introduced, where the operating area is limited to be at the right side of the Maximum Power Point (MPP) of the PV arrays (CPP-R). When PV systems experience a fast decrease in the irradiance, the robustness of the control algorithm decreases. The operating point may go to the open-circuit condition as shown in Fig. 2

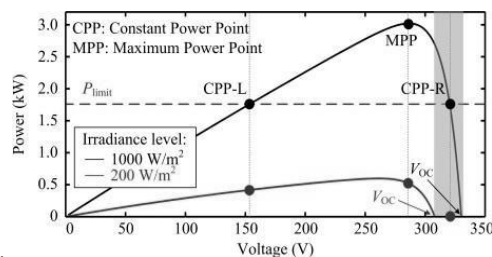


Fig. 2. Stability issues of the conventional CPG algorithms, when the operating point is located at the right side of MPP.

The above issues are resolved by extending the operating area of the P&O-CPG algorithm using two-stage grid connected PV system. By regulating the PV output power at the left side of the MPP (CPP-L), a stable CPG operation can be achieved, since the operating point will never “fall off the hill” during a fast decrease in the irradiance. Thus, the P&O-CPG algorithm can be applied to any two-stage single-phase grid connected PV system.

### 3. PROPOSED MODEL CONVENTIONAL CPG ALGORITHM

#### 3.1 System Configuration:

Fig.3 shows the basic hardware configuration of a two-stage single-phase grid-connected PV system and its control structure. The CPG control is implemented in the boost converter. The cascaded control of the full-bridge inverter is done where the DC-link voltage is kept constant through the control of the AC grid current, which is an inner loop. The PV system operates at a unity power factor, only when active power is injected to the grid. Here the two-stage configuration can extend the operating range of both the MPPT and CPG algorithms. In the two-stage case, the PV output voltage  $v_{pv}$  can be lower (i.e at the left side of the MPP), which is stepped up by using boost converter to match the required DC-link voltage.

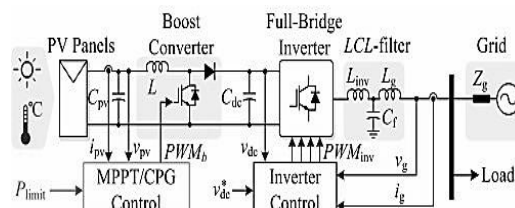


Fig. 3. Hardware schematic and overall control structure of a two-stage single phase grid-connected PV system.

#### 3.2 Operational Principle:

The operational principle of the conventional P&O- CPG algorithm is given in Fig 4. It operates into two modes: a) For MPPT mode ( $P_{pv} \leq P_{limit}$ ), the P&O algorithm should track the maximum power; b) For CPG mode ( $P_{pv} > P_{limit}$ ), the PV output power is limited at  $P_{limit}$ . The behavior of the algorithm is similar to the conventional P&O MPPT algorithm during the MPPT operation. The operating point will track and oscillate around the MPP. For CPG operation, the PV voltage  $v_{pv}$  is continuously perturbed toward a Constant Power Point (CPP), i.e.,  $P_{pv} = P_{limit}$ . The operating point will reach and oscillate around the CPP, after a number of iterations. Only the operation at the left side of the MPP (CPP-L) is considered for the stability concern, even if the PV system with the P&O-CPG control can operate at both CPPs. The control structure of the algorithm is shown in Fig 5. where  $v^*_{pv}$  can be expressed as

$$v^*_{pv} = \begin{cases} v_{MPPT}, & \text{when } P_{pv} \leq P_{limit} \\ v_{pv,n} - v_{step}, & \text{when } P_{pv} > P_{limit} \end{cases}$$

where  $v_{MPPT}$  is the reference voltage from the MPPT algorithm (i.e., the P&O MPPT algorithm),  $v_{pv,n}$  is the measured PV voltage, and  $v_{step}$  is the perturbation step size.

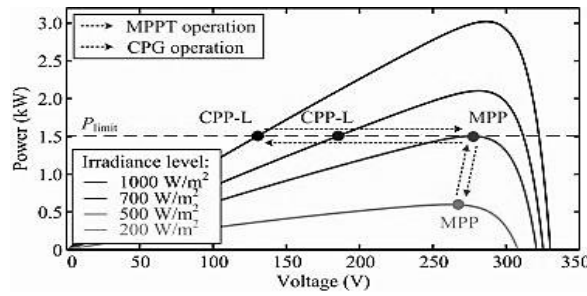


Fig. 4. Operational principle of the P&O-CPG algorithm with stability issues.

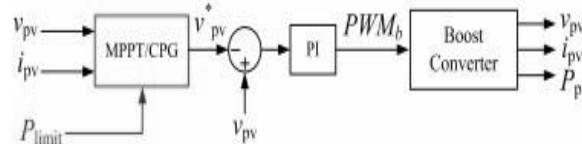


Fig. 5. Control structure of Algorithm with Proportional Integrator (PI).

**3.3 Issues of the P&O-CPG Algorithm:**

As shown in Fig 6.a, during a clear day, when the operating point is at the left side of the MPP, under slow changing irradiance conditions the P&O-CPG algorithm has a satisfied performance. However, in a cloudy day irradiance fluctuation will result in overshoots and power losses as shown in Fig 6.b. Assuming that the PV system is operating in MPPT mode initially and the irradiance level suddenly increases, the PV power  $P_{pv}$  increases by the change in the irradiance causing large power overshoots, as shown in Fig. 7 (i.e. A→B→C). Similarly, if the PV system is operating in the CPG operation (e.g., at CPP-L) and the irradiance suddenly drops, the output power  $P_p$  decreases suddenly, (i.e., C→D). The operating point reaches the new MPP (i.e., E) at that irradiance condition, after undergoing number of iterations, resulting in loss of power generation.

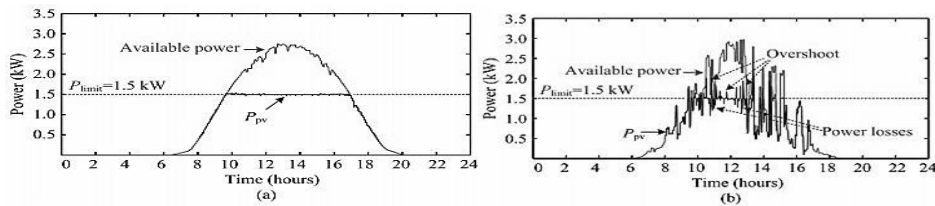


Fig. 6. Experimental result algorithm (P&O-CPG) under two daily conditions: (a) clear day and (b) cloudy day

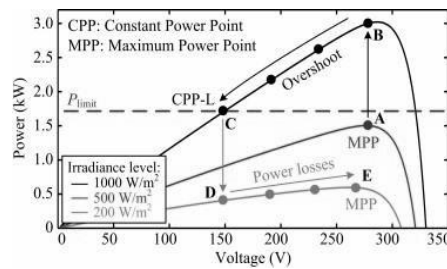


Fig. 7. Operating trajectory of the algorithm resulting in overshoot and power losses.

**A. Minimizing Overshoots**

Minimizing the overshoots as the tracking speed is increased is done by increasing the perturbation step size. Specifically, a large step size can reduce the required number of iterations to reach the corresponding CPP. When the algorithm detects a fast increase in the Irradiance Condition, only then step size modification can be enabled.

**B. Minimizing Power Losses**

When the CPG operating point is at the left side of the MPP, the P&O-CPG algorithm reaches the new MPP with a number of iterations during a fast decrease in irradiance, leading to power losses. There is not much change in operating point of the PV system if the PV system operates in the MPPT mode under different irradiance levels.

## 4. DESIGN PARAMETERS

### 4.1 Boost converters:

A boost converter is used to step up the DC output from PV panels, and the efficiency of interleaved boost converters can be improved using soft-switching techniques. These converters suffer switching losses, which can be reduced using **Zero-Current Switching (ZCS)** and **Zero-Voltage Switching (ZVS)** by incorporating resonant elements to make current or voltage zero during switching. ZCS eliminates turn-off losses but causes higher current stress and conduction losses, making it suitable for IGBTs. ZVS eliminates turn-on capacitive losses and is preferred for high-frequency operation, especially with MOSFETs. However, ZCS and ZVS are switching conditions, not specific control methods.

### 4.2 ZVT Boost Converter:

ZCS and ZVS achieve zero current or voltage only at specific switching instants, so some losses and ripples remain. To further improve efficiency, the Zero Voltage Transition (ZVT) topology is used, which ensures zero voltage across the switch during both turn-on and turn-off by adding auxiliary resonant components. This reduces switching losses without increasing stress on the switch, resulting in simpler control, higher efficiency, and performance improvement, with efficiency increasing from about 91% to nearly 97%.

Although ZVT is a commonly used technique, several ZVT has drawbacks such as:

- Turn-on capacitive losses at auxiliary switching,
- Main switch current stresses are higher,
- Also, higher auxiliary switch voltage stresses,
- Operation can be done under limited voltage converter ratio,
- Works with additional components count

To overcome these drawbacks, new ZVT topology is introduced as High step-up ZVT interleaved boost converter with WCCIs (Winding Cross Coupled Inductors) and reduced clamp switch number [8].

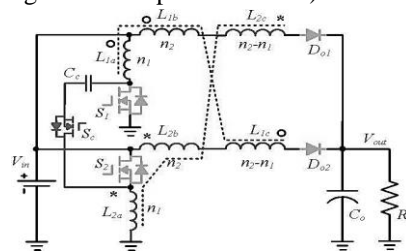


Fig. 8. ZVT interleaved boost converter with WCCIs (Winding Cross Coupled Inductors)

The topology is obtained from its isolated counterpart. Only one set of active clamp circuits containing a capacitor and an auxiliary switch is necessary for the interleaved two phases to suppress the voltage spikes and recycle the leakage energy. The switch voltage stress is reduced, and the voltage gain is extended. The reverse recovery problem of output diode is reduced by the leakage inductance. By adding two additional clamp capacitors  $Cd1$  ( $Cd2$ ), changing the turns of the third winding  $L1c$  ( $L2c$ ) from  $(n2-n1)$  to  $n2$ .

Converter has two coupled inductors each having three windings. The primary winding  $L1a$  is coupled to the second winding  $L1b$  and also it is coupled to the third winding  $L1c$  in another phase. Primary winding having turn  $n1$  and secondary and third winding has the turns as equal to  $n2$ .  $N$  is defined as the turns ratio of  $n2/n1$ . The coupled inductor 2 has the same structure. The coupling reference is pointed by “\*” marks and “o”. Using this converter the drawbacks get removed as follows:

- The switching losses are reduced in a great manner. The reverse recovery losses at the output diode are reduced greatly.
- ZVT soft switching performance is made for the main and the auxiliary switches due to the auxiliary commutation circuit.
- Reverse-recovery problem of output diode is minimized by the leakage inductance of the inductors connected in winding-coupled manner.

### 4.3 Topology modification with built-in LC low pass output filter:

The proposed ZVT interleaved DC–DC boost converter offers advantages over conventional interleaved boost converters for high step-up applications, but it also has some drawbacks. The leakage inductance of the coupled inductors and the parasitic capacitance of the output diodes form a resonant circuit during diode turn-off, causing voltage ringing and increased stress on the diodes. This leads to additional losses and reduced

efficiency. Moreover, the discontinuous current flowing into the output capacitor increases EMI noise and contributes to further parasitic losses. And the life of the electrolytic capacitor is getting shortened because of the discontinuous pulsed current. And by making some modification in topology the converter can be improved as [9],

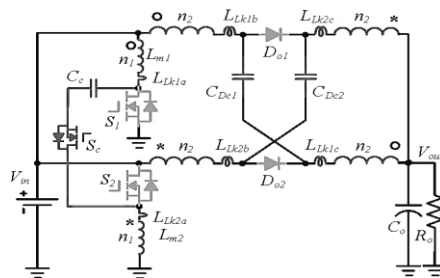


Fig. 9. Modified ZVT boost converter

The voltage ringing on the diode connected at output is regulated by the additional capacitors and built in low pass LC output filter. It is formed by the additional capacitors and the leakage inductance. So, the ripple in output current is cancelled and the EMI noises get reduced.

**4.4 Inverters:**

The boosted DC output of boost converter is converted into AC for further utilization by using inverters. Different topologies were included in the transformer-less grid connected PV system which improves the performance of inverters are as follows: -

- H5 topology
- HERIC topology (Highly efficient and Reliable Inverters Concept)
- H6 topology
- HB-ZVR topology (H-bridge zero voltage rectifier)
- PN-NPC topology (Neutral point clamped)
- Solidly clamped topologies-
  - a) NPC three level VSI
  - b) Dual parallel buck topology

Out of above topologies HERIC topology is the best topology with improved efficiency with using this topology. We can design very efficient inverter which controls the output of inverters that are fed to the grid or load. HERIC type inverter is also reliable in order to convert DC into AC with higher efficiency [10,12].

**4.5 Heric Inverter:**

The HERIC topology is shown in Fig. 10. The HERIC inverter where  $C_{dc}$  is DC-link capacitor,  $L_1$  and  $L_2$  are filter inductance at grid side and  $C_0$  is the filter capacitor. HERIC employs two extra switches on the ac side of inverter [10]. These additional switches have the two major functions: - isolating the photovoltaic panel from grid and preventing the reactive power exchange between the filter inductors and capacitors during the zero-voltage state, thus increasing efficiency. Also, the leakage current path is cut off as well.

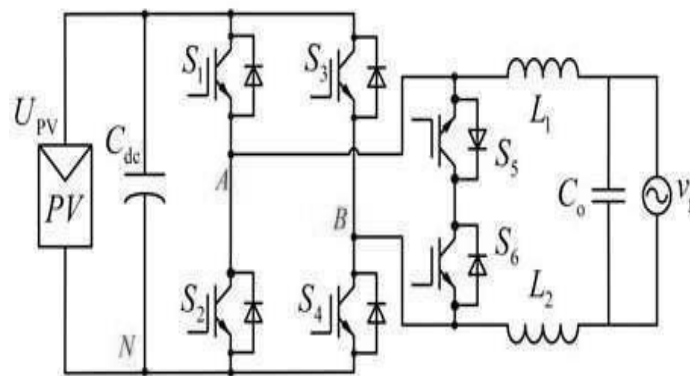


Fig. 10. HERIC Inverter

There are four operation modes. Fig shows that, in mode (1) S1, S4 switches conduct. In Mode (2) S5, S6 switches conduct. Same as in Mode (3) S2, S3 switches conduct and in Mode (4) S5, S6 switches conduct. Table of above 4 modes of operation can be given as follows –

Table -1: Mode of operation

Mode	Half Period	Conducting Devices	Vout
Active	Positive	S1, S4, S5	Vin
Free wheeling	Positive	S5, D6	0
Active	Negative	S2, S3, S6	-Vin
Free wheeling	Negative	D5, S6	0

During positive half cycle, known as active mode, where conducting devices S1, S4 and S5 are in conduction mode. S5 is in conduction to obtain active and zero vectors. The current flow through the path PV-S1-L1-L2-S4-PV. and freewheeling action takes place through S5 and D6 as shown in mode 2. positive vector appears across Vg i.e. Vout =Vin and during freewheeling action zero vector is obtained.[13].

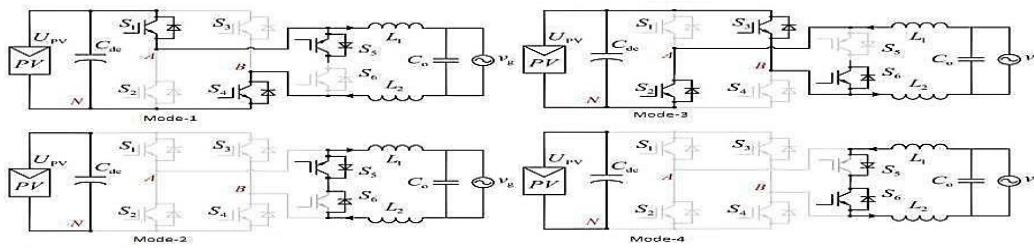


Fig. 11. Operation of HERIC inverter

During negative half cycle, conducting devices S2, S3 and S6 are in conduction mode as shown in mode 3. S6 is in conduction to obtain active and zero vectors. The current flow through the path PV-S3-L2-L1-S2-PV and freewheeling action take place through S6 and D5 as shown in mode 4. Negative vector appears across Vg i.e. Vout=-Vin and during freewheeling action zero vectors are obtained.

As shown in the graph below, three topologies are mentioned in terms of their efficiencies and power. The efficiencies of H5, HERIC, and H6 are 96.78%, 97%, and 97.09%, respectively.

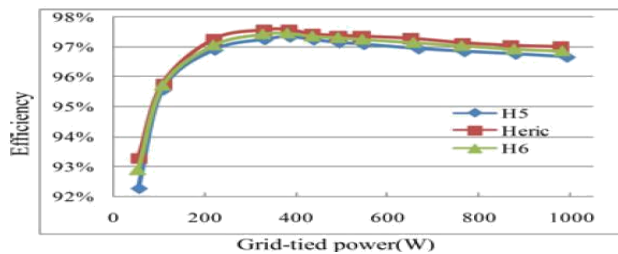


Fig. 12. Comparison by using graph

Even though H6 has high efficiency, conduction losses are more than that of HERIC and best thermal stress distribution than that of H6. So, we can conclude that HERIC topology is the best for INVERTERS. Selection of desired MPPT: The major characteristics of all MPPT techniques are summarized in one table which gives better understanding with simplicity and comparative analysis. Only those techniques which are applicable for efficient and reliable operation of PV system can be chosen.

4.6 Perturb & Observe (P & O):

P&O is widely used due to easy implementation. This technique forces the PV system to approach MPP by increasing or decreasing the panel output voltage.

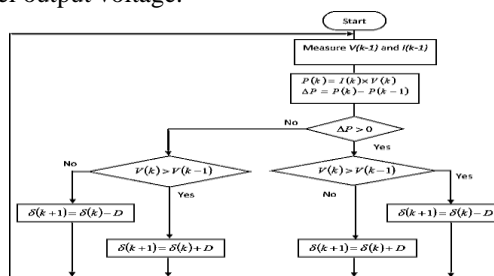


Fig. 13. Flowchart

To check direction, change in maximum power, the P&O method perturbs the operating voltage of PV panel. There are two conditions:

- 1) When power increases; operating voltage perturbs in same direction.
- 2) When power decreases; operating voltage perturbs in reverse direction. This process will continue until MPP is reached. The oscillations around MPP are minimized by reducing perturbation step size. MPPT techniques and having good performance characteristics are generally used. When we take parameters into account like efficiency, implementation, sensor, cost and applications etc. P&O is one of the best conventional techniques.

**Table -3:** Different MPPT techniques

MPPT Technique	PV Array Dependent	True MPPT	Analog or Digital	Periodic Tuning	Convergence Speed	Implementation Complexity	Sensed Parameter
1.Hill-climbing / P & O	No	Yes	Both	No	Varies	Low	Voltage, Current
2.Incremental conductance	NO	Yes	Digital	No	Varies	Medium	Voltage, Current
3.Fractional Voc	Yes	No	Both	Yes	Medium	Low	Voltage
4.Fractional Isc	Yes	No	Both	Yes	Medium	Medium	Current
5.Fuzzy Logic Control	Yes	Yes	Digital	Yes	Fast	High	Varies
6.Neural network	Yes	Yes	Digital	Yes	Fast	High	Varies
7.RCC	No	Yes	Analog	No	Fast	Low	Voltage, Current
8.Current sweep	Yes	Yes	Digital	Yes	Slow	High	Voltage, Current
9.DC link capacitor droop control	No	No	Both	No	Medium	Low	Voltage
10.Load I V Maximization	No	No	Analog	No	Fast	Low	Voltage, Current
11. $dp/dv$ or $dp/di$ Feedback Control	No	Yes	Digital	No	Fast	Medium	Voltage, Current
12.Array Reconfiguration	Yes	No	Digital	Yes	Slow	High	Voltage, Current
13.Linear current control	Yes	No	Digital	Yes	Fast	Medium	Irradiance
14. $I_{mpp}$ or $V_{mpp}$ computation	Yes	Yes	Digital	Yes	N/a	Medium	Irradiance, Temp.
15.State based MPP	Yes	Yes	Both	Yes	Fast	High	Voltage, Current
16.OCC MPPT	Yes	No	Both	Yes	Fast	Medium	Current
17.BFV	Yes	No	Both	Yes	N/A	Low	None
18.LRCM	Yes	No	Digital	No	N/A	High	Voltage, Current
19.Slide Control	No	Yes	Digital	No	Fast	Medium	Voltage, Current

## 5. CONCLUSION

The proposed control strategy ensures stable constant power generation by operating the PV system on the left side of the maximum power point, enabling smooth transitions and improved stability compared to traditional methods. Experimental results show reduced overshoot, lower power losses, and fast dynamic response. With a limited PV voltage range and minor algorithm adjustments, stable operation is maintained. Using a ZVT boost

converter and HERIC inverter, the energy transmission efficiency can be increased to about 98% and 97%, respectively.

## 7. REFERENCE

- [1] T. Stetz, F. Marten, and M. Braun, "Improved low voltage grid integration of photovoltaic systems in Germany," *IEEE Trans. Sustain. Energy*, vol. 4, no. 2, pp. 534–542, Apr. 2013.
- [2] A. Ahmed, L. Ran, S. Moon, and J.-H. Park, "A fast PV power tracking control algorithm with reduced power mode," *IEEE Trans. Energy Conversion*, vol. 28, no. 3, pp. 565–575, Sept. 2013.
- [3] Y. Yang, H. Wang, F. Blaabjerg, and T. Kerekes, "A hybrid power control concept for PV inverters with reduced thermal loading," *IEEE Trans. Power Electron.*, vol. 29, no. 12, pp. 6271–6275, Dec. 2014.
- [4] German Federal Law: Renewable Energy Sources Act (Gesetz für den Vorrang Erneuerbarer Energien) BGBl, Std., July 2014.
- [5] R. G. Wandhare and V. Agarwal, "Precise active and reactive power control of the PV-DGS integrated with weak grid to increase PV penetration," in *Proc. of PVSC*, pp. 3150–3155, Jun. 2014.
- [6] F. Blaabjerg, R. Teodorescu, M. Liserre, and A. V. Timbus, "Overview of control and grid synchronization for distributed power generation systems," *IEEE Trans. Ind. Electron.*, vol. 53, no. 5, pp. 1398–1409, Oct. 2006.
- [7] T. Eram and P. L. Chapman, "Comparison of photovoltaic array maximum power point tracking techniques," *IEEE Trans. Energy Conversion*, vol. 22, no. 2, pp. 439–449, Jun. 2007.
- [8] "A Review of Non-Isolated High Step-Up DC/DC Converters in Renewable Energy Applications." Wuhua Li, Xiaodong Lv, Yan Deng, Jun Liu, Xiangning He
- [9] "Interleaved ZVT Boost Converters with Winding-Coupled Inductors and Built-In LC Low Pass Output Filter Suitable for Distributed Fuel Cell Generation System." Wuhua Li, Yan Deng, Rui Xie, Jianjiaing Shi, Xiangning He.
- [10] "H6 Transformer less Full-Bridge PV Grid-tied Inverters." Li Zhang, *Member, IEEE*, Kai Sun, *Member, IEEE*, Yan Xing, *Member, IEEE* and Mu Xing
- [11] "Single Phase Transformer Less Grid Connected PV Inverter" Carmaline Joel Anthony, Sigatoka, S. P. Muley
- [12] "Different Type of Inverter Topologies for PV Transformer less Standalone System" Chirag Sinh Raj, Mr. Hitesh Lade
- [13] "Design of HERIC Configuration Based Grid Connected Single Phase Transformer Less Photovoltaic Inverter" Payal Somani, Divyesh J. Vaghel